Journal of Power Sources 195 (2010) 2064–2068

Contents lists available at ScienceDirect

Journal of Power Sources

journal homepage: www.elsevier.com/locate/jpowsour

Short communication

Synthesis and electrochemical evaluation of an amorphous titanium dioxide derived from a solid state precursor

Christopher D. Joyce[a], Toni McIntyre[b], Sade Simmons[b], Holly LaDuca[a], Jonathan G. Breitzer[b], Carmen M. Lopez[a], Andrew N. Jansen[a], J.T. Vaughey[a,*]

[a] Electrochemical Energy Storage Group, Chemical Sciences and Engineering Division, Argonne National Laboratory, 9700 S Cass Ave., Argonne, IL 60439, United States
[b] Department of Natural Science, Fayetteville State University, Fayetteville, NC, United States

ARTICLE INFO

Article history:
Received 25 August 2009
Received in revised form 16 October 2009
Accepted 19 October 2009
Available online 30 October 2009

Keywords:
Titanium dioxide
Precursor
Electrochemistry
Anode

ABSTRACT

Titanium oxides are an important class of lithium–ion battery electrodes owing to their good capacity and stability within the cell environment. Although most Ti(IV) oxides are poor electronic conductors, new methods developed to synthesize nanometer scale primary particles have achieved the higher rate capability needed for modern commercial applications. In this report, the anionic water stable titanium oxalate anion $[TiO(C_2O_4)_2]^{2-}$ was isolated in high yield as the insoluble DABCO (1,4-diazabicyclo[2.2.2]octane) salt. Powder X-ray diffraction studies show that the titanium dioxide material isolated after annealing in air is initially amorphous, converts to N-doped anatase above 400 °C, then to rutile above 600 °C. Electrochemical studies indicate that the amorphous titanium dioxide phase within a carbon matrix has a stable cycling capacity of ~350 mAh g^{-1}. On crystallizing at 400 °C to a carbon-coated anatase the capacity drops to 210 mAh g^{-1}, and finally upon carbon burn-off to 50 mAh g^{-1}. Mixtures of the amorphous titanium dioxide and $Li_4Ti_5O_{12}$ showed a similar electrochemical profile and capacity to $Li_4Ti_5O_{12}$ but with the addition of a sloping region to the end of the discharge curve that could be advantageous for determining state-of-charge in systems using $Li_4Ti_5O_{12}$.

1. Introduction

Titanium dioxide is an important material used in many industrial and scientific applications. In addition to several naturally occurring polytypes, e.g. brookite, anatase, and rutile, several man-made polymorphs have been synthesized via ion-exchange, notably TiO_2(B) from $K_2Ti_4O_9$ and TiO_2(H) from $K_2Ti_8O_{16}$ [1–13]. The polytype isolated is dependant on variables that include the precursor, temperature and atmosphere utilized. Low temperature preparations (<100 °C) yield brookite, samples above 700 °C yield rutile, and anatase is isolated between these temperatures. For samples prepared or annealed under an ammonia atmosphere, nitrogen-doped yellow anatase or rutile has been isolated and characterized [14,15]. As bulk materials, rutile is electrochemically inactive, brookite inserts 0.16 Li per formula unit, anatase and TiO_2(H) and TiO_2(B) insert 0.5 Li per formula unit [1,2,7,10]. These differences reflect the different arrangements of the titanium centered octahedra within the material and the resultant internal void space. Significant differences and levels of activity have been reported when the nanoscale versions of the materials are evaluated reflecting the smaller diffusion distances and increasing important role of surfaces [16–18].

In this paper we report the synthesis and characterization of the air and water stable titanium dioxide precursor compound $(H_2DABCO)(TiO(C_2O_4)_2)\cdot 2H_2O$, its decomposition products, and the electrochemical evaluation of the various titanium dioxides produced by annealing this material in air.

2. Experimental

The synthesis of titanyl-oxalato anion, $[TiO(C_2O_4)_2\cdot xH_2O]^{2-}$, has been reported in the literature starting from the slow hydrolysis of $TiCl_4$ [19]. Due to the problems associated with working with titanium tetrachloride, the synthesis was modified to use titanium isopropoxide, $Ti(OC_3H_8)_4$ (Aldrich, 97%). In a typical synthesis, 50 ml of NH_4OH (Aldrich, 29.2% solution) was added to 25 ml of $Ti(OC_3H_8)_4$, producing a white gelatinous precipitate. The precipitate was washed three times to remove excess base and placed in 100 ml of de-ionized water. To this solution 200 ml of a 0.23 M solution of oxalic acid (Aldrich, 99.9%) were added producing a clear solution of $H_2[TiO(C_2O_4)_2]$. To this, a stoichiometric amount of an aqueous solution of DABCO (1,4-diazabicyclo[2.2.2]octane) (Aldrich,98%) were added precipitating a while crystalline solid.

* Corresponding author. Tel.: +1 063025208885; fax: +1 06302524716.
E-mail address: vaughey@anl.gov (J.T. Vaughey).

0378-7753/$ – see front matter © 2009 Elsevier B.V. All rights reserved.
doi:10.1016/j.jpowsour.2009.10.061

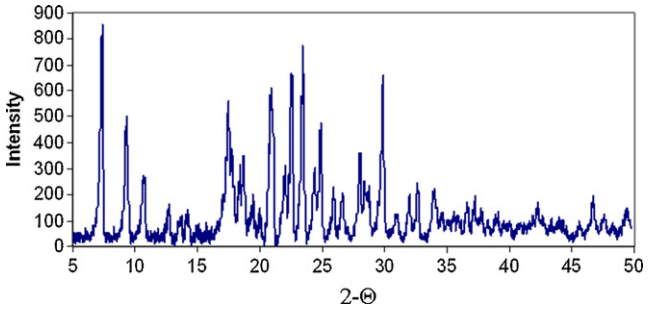

Fig. 1. The powder X-ray diffraction pattern of $(H_2DABCO)(TiO(C_2O_4)_2)\cdot 2H_2O$.

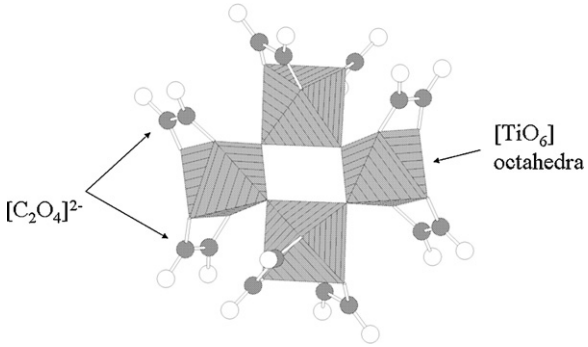

Fig. 2. Tetramer of $(TiO(C_2O_4)_2)^{2-}$ anion from $K_2(TiO(C_2O_4)_2)\cdot 2H_2O$ (Ref. [23]). The small grey spheres are the oxalate carbons, the open spheres the oxalate oxygen's, and the hatched polyhedra are $[TiO_6]$.

Thermogravimetric analysis (TGA) was performed using a Seiko X-star 6300 TGA/DTA. Data were collected under flowing dry air atmosphere to determine water content and the temperature of decomposition for the material. The structures of the compounds isolated were determined by annealing the precursor at a variety of temperatures under air and characterizing by powder X-ray diffraction methods. Data collected on a Siemens D5000 Powder X-ray Diffractometer were used to determine the type and purity of the titanium dioxide produced.

Electrochemical evaluation of select titanium dioxide samples isolated was performed. Electrodes were laminated on aluminum foil using a mixture of 80% active, 10% PvDF binder, and 10% acetylene black as a conductive additive. The electrodes were used to build 2032-type cells and evaluated using a lithium metal anode and a 1.2 M $LiPF_6$ in 3:7 EC:EMC electrolyte [20]. Cells were cycled in the range 0.7–4.2 V using a constant current (0.08 mA or 0.05 mA cm^{-2}) on a MACCOR cycler. In addition, a mixture of the amorphous titanium dioxide (350 °C) was blended (1:2) with a commercial sample of $Li_4Ti_5O_{12}$ and evaluated in the voltage window of 1.0–2.0 V (at 0.05 mA cm^{-2}).

Scanning electron microscopy (SEM) images were acquired utilizing an FEI Quanta 400 FEG Scanning Electron Microscope operating at 12.5 kV, under high vacuum mode. The SEM images were recorded with the Quanta xT microscope control software, version 2.4. Prior to image acquisition, the samples were sputter-coated using a Bal-Tec MED020 sputter coater with 10 nm of Au/Pd to prevent charging.

3. Results and discussion

Building on our previous work developing low temperature preparations for electrochemically active titanium oxides, we sought to develop an air stable microcrystalline single source precursor to nanoscale titanium dioxide [19]. In addition to electrochemical interest, such a precursor would be useful as a source of active titanium dioxide for the synthesis of various titanium-based materials where the particle morphology needs to be maintained. For electrode materials based on titanium (IV) oxides, numerous studies have shown that doping or reducing the particle size of the titanium dioxide, significantly increases the rate capability [1,15,21]. However synthetic procedures starting from the simple dioxide usually require a high temperature heating step (with resulting loss of surface area) that may lead to an undesirable side reaction with the reaction vessel, or for battery materials evaporation of lithia.

In our study, a solution of the titanyl-oxalato anion was prepared starting from titanium isopropoxide. To the clear solution of the acid version of the anion, addition of the large organic cation DABCO (1,4-diazabicyclo[2.2.2]octane) was found to precipitate the titanyl-oxalato anion as the salt $(H_2DABCO)(TiO(C_2O_4)_2\cdot xH_2O)$. The powder pattern is shown in Fig. 1. Earlier crystallographic studies by Fester et al., on the potassium salt showed the anion existed as a tetramer in the solid state, shown in Fig. 2 [22,23]. Addition of other divalent countercations, such as Mn(II) or Ni(II), resulted in decomposition and precipitation of the simple oxalate salt, $M(C_2O_4)\cdot H_2O$, while alkali metal salts were too soluble and were isolated by solvent evaporation [19,22].

The decomposition of the $(H_2DABCO)(TiO(C_2O_4)_2)\cdot xH_2O$ salt was studied by thermogravimetric analysis (TGA) under an air atmosphere. The data, shown in Fig. 3, indicated a 10% weight loss around 100 °C, a large weight loss (45%) at 275 °C, and a slow weight loss, completed by 500 °C, that corresponded to 25% of the overall total. The weight loss at 100 °C corresponds to 2.0 waters of hydration, the sharp drop at 275 °C is mainly from the oxalate fragments, and the final weight loss is close to that expected from the DABCO cation.

The crystalline products of the decomposition were determined by heating of the salt at eight temperatures between 300 and 900 °C in air for 12 h. Samples heated below 400 °C sample were found to be amorphous to X-ray diffraction methods. The materials isolated were black in color owing to the carbon produced from the incomplete decomposition of the DABCO cation. The 400 and 500 °C samples were found to be single phase anatase. Scherrer equation calculations indicated a primary particle size of approximately 500 nm for both materials. The 400 °C sample was black and the 500 °C sample yellow. The samples heated above 600 °C materials were white. The 600 °C sample contained mainly rutile with a few percent anatase, while the 900 °C product had rutile as the only product. The XRD patterns are shown in Fig. 4.

Fig. 5 shows the SEM images of a typical 350 °C sample (Fig. 5a, left), and a typical 500 °C sample (Fig. 5b, right). Both samples show similar morphology, i.e. roughly rectangular and flat particles fused together to form larger particles of irregular shape. The average particle size of the secondary particles for the 350 °C sample is approximately 50% larger (~30 μm), than the 500 °C sample (~20 μm). The inset shows an enlargement of the 500 °C particles highlighting the overall plate-like morphology. The reduced particle size for the sample heated to higher temperature likely

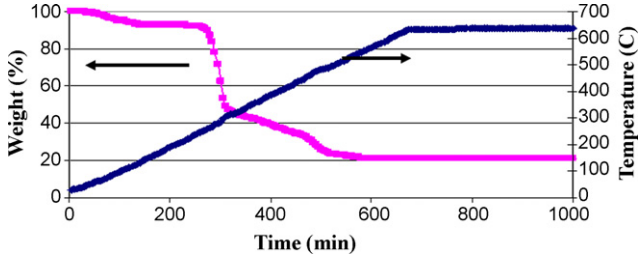

Fig. 3. The TGA pattern for $(H_2DABCO)(TiO(C_2O_4)_2)\cdot 2H_2O$.

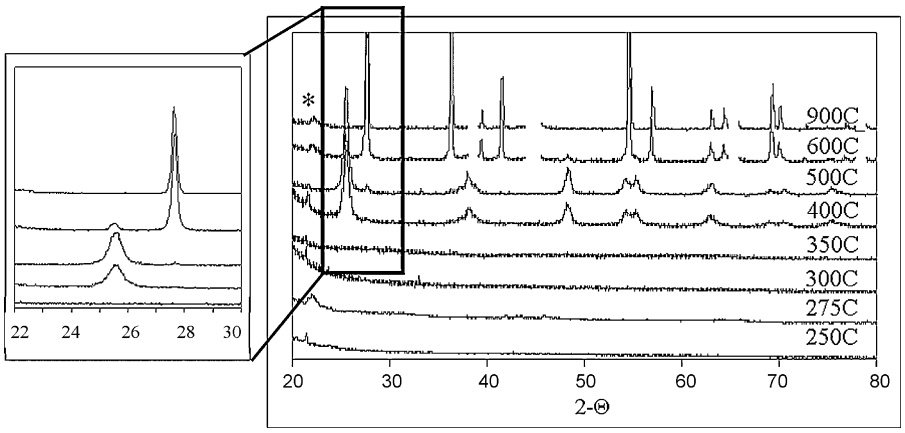

Fig. 4. Stacked XRD patterns of the TiO_2 produced by the decomposition of $(H_2DABCO)(TiO(C_2O_4)_2)\cdot 2H_2O$ at different temperatures. Sample holder peaks have been removed for clarification and carbon is marked with an asterisk. The inset shows the transition from anatase to rutile with increasing temperature.

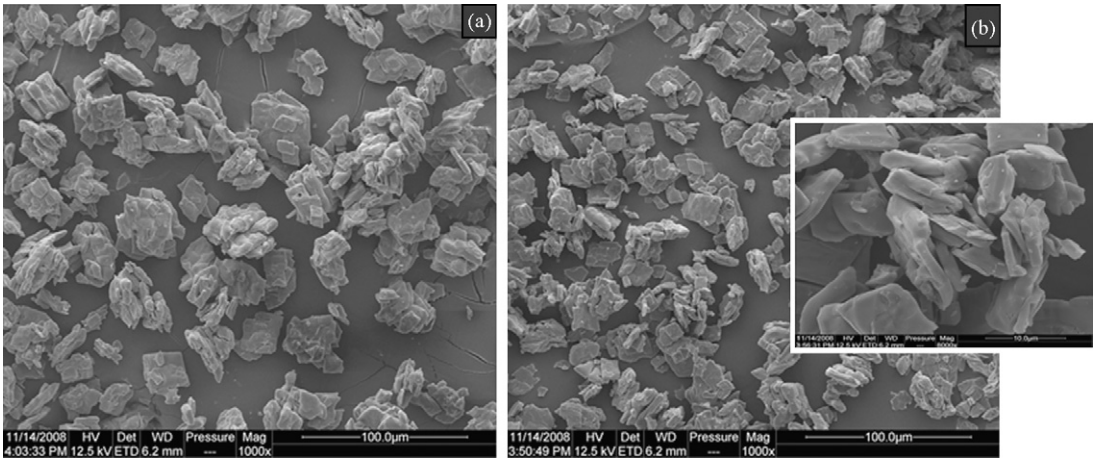

Fig. 5. SEM images of the amorphous TiO_2 (350 °C, left) and the N-doped TiO_2 (500 °C, right). The inset shows an enlarged picture of the 500 °C particles and their morphology.

reflects the particle breakdown that occurred upon completion of the decomposition of the DABCO cation (as seen in the TGA data) and the loss of remaining organic compounds.

Numerous titanium oxides and lithium titanium oxides are currently under study as next generation anodes for lithium ion batteries [3,7]. Studies have shown that for titanium oxides, reducing the particle size do not decrease safety but does increase rate capability and in some instances capacity [1,6,13,14,24,25]. The amorphous sample (350 °C) and the anatase samples (400, 500 °C, commercial sample) were evaluated electrochemically and the data is shown in Fig. 6. Of the samples evaluated, the 350 °C amorphous sample showed the highest stable cycling capacity, ~350 mAh g^{-1}, equal to 1.0 Li/TiO_2, taking into account the carbon residue from the incomplete decomposition of the precursor salt. As isolated

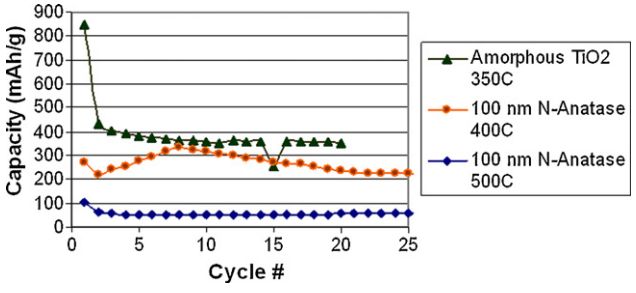

Fig. 6. Cycling performance of the various nanoscale TiO_2 materials isolated.

the material is a mixture of 55 wt% carbon and 45 wt% TiO_2 whose capacity is approximately 160 mAh g^{-1}. The cycling capacity of the anatase (400 °C) sample stabilized at 210 mAh g^{-1}, while the 500 °C sample yielded 50 mAh g^{-1}. A comparison of the cycling profiles for the amorphous titanium dioxide and anatase (500 °C) is shown in Fig. 7. The 500 °C sample has the ~2.0 V insertion plateaus characteristic of anatase, while the amorphous sample lacks these features. The lack of plateaus (even on cycling) and powder XRD data is consistent with the lack of a crystalline anatase component to the amorphous material. The observed capacity of the amorphous TiO_2/carbon mixture, mainly between 1 and 2 V vs. lithium, is comparable to $Li_4Ti_5O_{12}$ and if used as a mixture could act as a state-of-charge indicator for the electrode by adding a slight slope to the discharge curve [20,21]. This effect is shown in Fig. 8, where the figure on top shows the cycling profile of the blend, while the bottom figure is $Li_4Ti_5O_{12}$ alone.

It can be readily seen that on heating to 400 °C, the amorphous TiO_2 component of the amorphous phase crystallizes to anatase resulting in a drop in cycling capacity. This capacity difference, taken as the TiO_2 component alone, is consistent with the reported capacity of anatase. Based on the TGA data, the 350 °C sample is ~55% carbon, while the 400 °C sample is ~40% carbon. The 500 °C sample has no additional carbon. The high irreversible capacity of the amorphous sample (~50%) probably arises from lithium reduction of the partially reduced organic components.

The drop in capacity between the carbon-coated anatase (400 °C) and the N-doped anatase (500 °C) is large—nearly 75%.

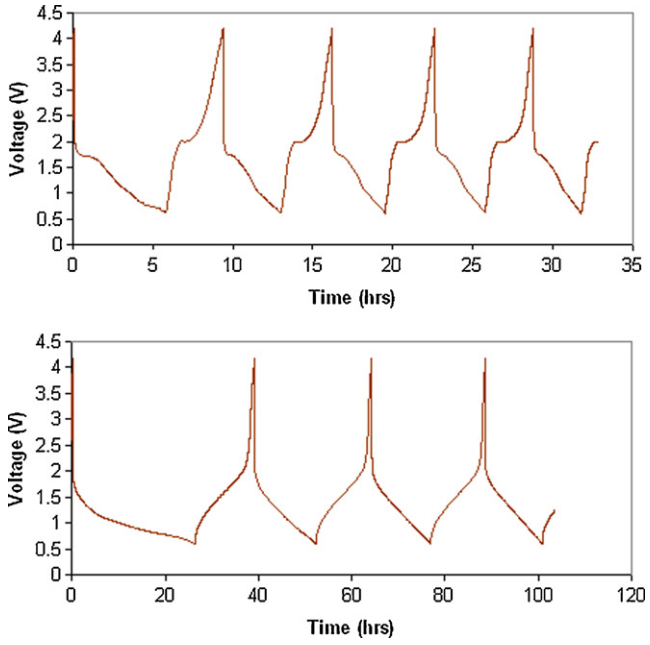

Fig. 7. Cycling profiles of anatase TiO_2 produced at 500 °C (top) and the amorphous TiO_2 sample from 350 °C (bottom).

Although the sample appears to have the typical cycling profile of anatase, it is not being completely utilized after burn-off of the carbon coating from the DABCO cation. It is possible that this 500 °C TiO_2 sample has poor ionic conductivity owing to the presence of nitrogen anions in the lattice and charge compensating protons in the central channel [26]. In a situation similar to the olivine cathode material $LiFePO_4$, poor lithium conductivity is the stoichiometric uncoated material results in a low cycling capacity [27]. Numerous studies on carbon coating the material, ex situ or in situ, show that as little as a few percent carbon properly applied can result in realization of full theoretical capacity [28,29].

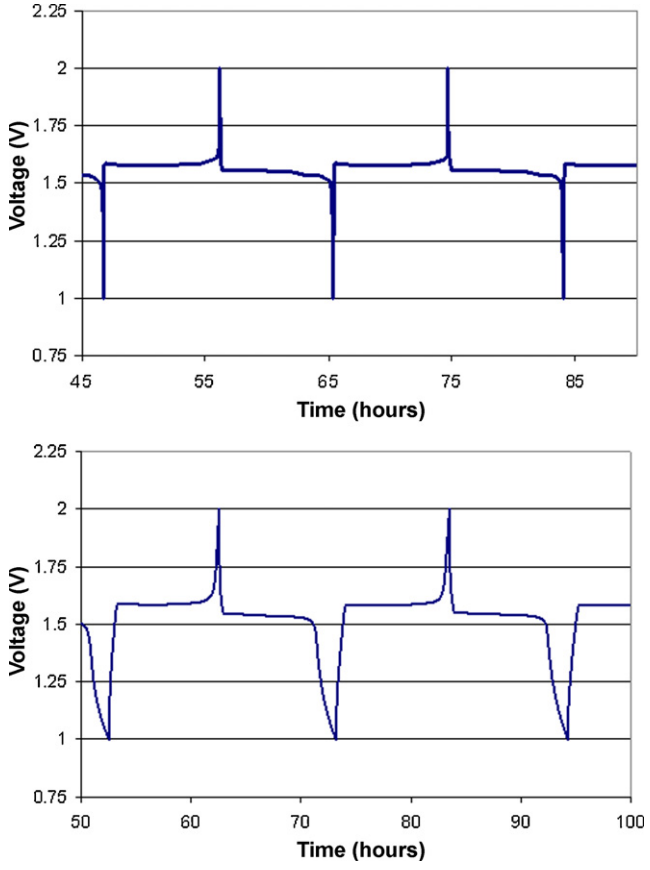

Fig. 8. Two cycles of (top) a 1:2 blend of the amorphous TiO_2 and $Li_4Ti_5O_{12}$ and (bottom) $Li_4Ti_5O_{12}$ alone.

4. Conclusion

A new air and water stable titanium dioxide precursor has been developed, characterized, and its decomposition products evaluated as electrode materials. Initial studies on the salt $(H_2DABCO)(TiO(C_2O_4)_2)\cdot 2H_2O$ show decomposition to an amorphous material below 400 °C with very good electrochemical activity alone and in a blend with $Li_4Ti_5O_{12}$. The crystalline titanium dioxide materials isolated at higher temperatures showed overall poorer electrochemical performance when compared to commercial or literature samples, possibly due to interstitial atoms blocking the main diffusion channel.

Acknowledgments

The authors would like to thank Ms. Anna Baebler and Dr. Chris Johnson for their assistance. The research was performed, in part, at Argonne National Laboratory as a research participant in the FaST Program. The program is administered by Argonne's Division of Educational Programs with funding provided by the U.S. Department of Energy and the National Science Foundation's North Carolina Louis Stokes Alliance for Minority Participation. Support to conduct this work came from the Office of Vehicle Technologies (Batteries for Advanced Transportation Technologies (BATT) Program) of the U.S. Department of Energy under Contract No. DE-AC02-06CH11357 and is gratefully acknowledged.

References

[1] M.A. Reddy, V. Pralong, U.V. Varadaraju, B. Raveau, Electrochem. Solid State Lett. 11 (2008) A132.
[2] J. Wang, J. Polleux, J. Lim, B.J. Dunn, Phys. Chem. C 111 (2007) 14925.
[3] P.G. Bruce, B. Scrosati, J.-M. Tarascon, Angew. Chem. Int. Ed. 47 (2008) 2930.
[4] A.S. Arico, P.G. Bruce, B. Scrosati, J.-M. Tarascon, W. van Schalkwijk, Nat. Mater. 4 (2005) 366.
[5] G. Sudant, E. Baudrin, D. Larcher, J.-M. Tarascon, J. Mater. Chem. 15 (2005) 1263.
[6] M. Fernandez-Garcıa, C. Belver, J.C. Hanson, X. Wang, J.A. Rodriguez, J. Am. Chem. Soc. 129 (2007) 13604.
[7] R.A. Armstrong, G. Armstrong, J. Canales, R. Garcia, P.G. Bruce, Adv. Mater. 17 (2005) 862.
[8] C.H. Jiang, M.D. Wei, Z.M. Qi, T. Kudo, I. Honma, H.S. Zhou, J. Power Sources 166 (2007) 239.
[9] M. Latroche, L. Brohan, R. Marchand, M. Tournoux, J. Solid State Chem. 31 (1989) 78.
[10] L.D. Noailles, C.S. Johnson, J.T. Vaughey, M.M. Thackeray, J. Power Sources 81–82 (1999) 259.
[11] Y.S. Hu, L. Kienle, Y.G. Guo, J. Maier, Adv. Mater. 18 (2006) 1421.
[12] M.A. Reddy, M.S. Kishore, V. Pralong, U.V. Varadaraju, B. Raveau, Electrochem. Solid State Lett. 10 (2007) A29.
[13] M.A. Reddy, M.S. Kishore, V. Pralong, V. Caignaert, U.V. Varadaraju, B. Raveau, Electrochem. Commun. 8 (2006) 1299.
[14] C. Di Valentin, G. Pacchioni, A. Selloni, S. Livraghi, E. Giamello, J. Phys. Chem. B 109 (2005) 11414.
[15] K.S. Rane, R. Mhalsiker, S. Yin, T. Sato, K. Cho, E. Dunbar, P. Biswas, J. Solid State Chem. 179 (2006) 3033.
[16] S. Nordlinder, L. Nyholm, T. Gustafsson, K. Edström, Chem. Mater. 18 (2006) 495.
[17] X. Li, Y. Xiong, Z. Li, Y. Xie, Inorg. Chem. 45 (2006) 3493.
[18] Y.V. Kolen'ko, A.A. Burukhin, B.R. Churagulov, N.N. Oleinikov, Inorg. Mater. 40 (2004) 822.
[19] E.M. Sorenson, S.K. Barry, H.K. Jung, J.R. Rondinelli, J.T. Vaughey, K.R. Poeppelmeier, Chem. Mater. 18 (2006) 482.
[20] C.D. May, J.T. Vaughey, Electrochem. Commun. 6 (2005) 1075.

[21] C.H. Chen, J.T. Vaughey, A.N. Jansen, D.W. Dees, A.J. Kahaian, T. Goacher, M.M. Thackeray, J. Electrochem. Soc. 148 (2001) A102.
[22] A. Fester, W. Bensch, M. Trömel, Inorg. Chim. Acta 193 (1992) 99.
[23] A. Fester, W. Bensch, M. Trömel, Acta Crystallogr. C 50 (1994) 850.
[24] X.L. Yao, S. Xie, C.H. Chen, Q.S. Wang, J.H. Sun, Y.L. Li, S.X. Lu, Electrochim. Acta 50 (2005) 4076.
[25] H. Furukawa, M. Hibino, I. Honma, J. Electrochem. Soc. 151 (2004) A527.
[26] M.-C. Tsai, J.-C. Chang, H.-S. Sheu, H.-T. Chiu, C.-Y. Lee, Chem. Mater. 21 (2009) 499.
[27] A.K. Padhi, K.S. Nanjunadaswamy, J.B. Goodenough, J. Electrochem. Soc. 144 (1997) 1188.
[28] M.M. Doeff, Y.Q. Yu, F. McLarnon, R. Kostecki, Electrochem. Solid State Lett. 6 (2003) A207.
[29] C.R. Sides, F. Croce, V. Young, C.R. Martin, B. Scrosati, Electrochem. Solid State Lett. 8 (2005) A484.